

UNSTEADINESS OF THE ROTOR SLIPSTREAM IN THE GROUND EFFECT AND ITS IMPACT ON HELIPAD LOADS

Pawel Ruchala, pawel.ruchala@ilot.edu.pl, Łukasiewicz Research Network – Institute of Aviation (Poland)

Abstract

The concept of elevated (rooftop) heliport is known and developed for decades. However due to the significant noise and other drawbacks of helicopters, their application in practice is currently limited mostly to emergency cases, like the lifesaving. Secondly, in recent years the idea of autonomic, light and quiet air taxis flying to cities gains in interests. Such vehicles would need some amount of free space to land and take-off safely; the rooftop heliports seem to be perfectly suitable.

A drawback of the elevated heliports may be vibrations of the whole building, caused primarily by the unsteadiness of the rotor slipstream impinging on the heliport surface during take-off and landing. It is especially awkward in case of medical heliports, due to strict vibration requirements. On the other hand, oscillations of loads caused by a helicopter rotor slipstream are quite unappreciated issue. To investigate this topic, an experimental investigation focused on a remotely controlled, 450-class helicopter, has been performed. Measurement of pressure acting on the simulated heliport plate showed a level of pressure oscillations for different test cases, as a function of radial position. The Fourier analysis has also been performed to show dominant frequency of the oscillation. Moreover, the velocity field in the rotor slipstream was captured using PIV method to capture the tip vortices position, to explain the low-frequency component of the oscillation.

1. INTRODUCTION

1.1. Application of elevated heliports

The far-reaching objective of presented paper is to discuss the unsteadiness of helicopter's rotor slipstream in the proximity of ground. The unsteady aerodynamic forces caused by the slipstream are considered as the main source of vibration of the landing pad below the helicopter, next to a motion from the engine and rotors and by an impact from the landing itself^[9]. The topic of helipad vibration may be found unimportant in case of ground-level helipad. Meanwhile, it is opposite if the helicopter operates from an elevated helipad – especially considering that a vast majority of such helipads are currently used in medical applications. It is well known fact that medical rooms, amongst others the surgeries, have much more strict requirements, than offices, apartments etc.^[7]. The rapid growth of interests in medical helipads triggered an investigation of some issues related with them, e.g.^{[2]; [3]; [10]}. Secondly, in recent years the Urban Air Mobility concept gains in interests. This idea foresees an application of autonomic, light, and quiet multicopters as air taxis flying to cities. One may observe that it seems to be a reminiscence of similar concepts covering helicopters, developed in 40's or 50's. It is believed that the drawback of rotorcrafts will be significantly reduced in comparison to classic helicopters. Use of electric motors, instead of turbines, should reduce the noise level – similarly, like reduction of rotors diameter. The latter feature should also improve the safety, as

the mass and kinetic energy of each rotor is reduced. So, if e-VTOLs will become popular in this kind of transport, they likely will need some amount of free space in densely built city centers, which would be used to safe landing and convenient change. For that purpose, elevated heliports seem to be more suitable, than ground-level ones.



Fig. 1. Elevated helipad in hospital in Olsztyn, Poland

Despite the concept of elevated heliport is roughly as old, as helicopter itself, the knowledge about its vibrations caused by the rotor slipstream seems to be incomplete. Among others, there is a lack of information about the magnitude of oscillation and parameters, which have the greatest impact on it. It may be explained by a fact that the design of an elevated heliport is relatively complex, as it cannot be treated as a standalone add-on to a project. In fact, it is very intimately interlinked – sometimes in surprising ways – with rest of the project^[9].

1.2. Structure of slipstream

The flow field around a helicopter hovering at low altitude above the ground (in ground effect, IGE) seems to be well known. In this case the slipstream impinges on the ground and flows out horizontally, out of the rotor. In the structure of the slipstream of a helicopter rotor in the ground effect (IGE) one can distinguish four regions [8], as it has been presented in Fig. 2:

1. Contraction, where the slipstream velocity is directed more or less vertically – similar to the OGE (out of ground effect) case;
2. Transition, where interaction with the ground turns the flow to the horizontal direction along the ground
3. Outwash, where the flow is directed along the ground and its peak value decays with increase in radial distance
4. Recirculation, where the flow is induced by the slipstream due to air viscosity

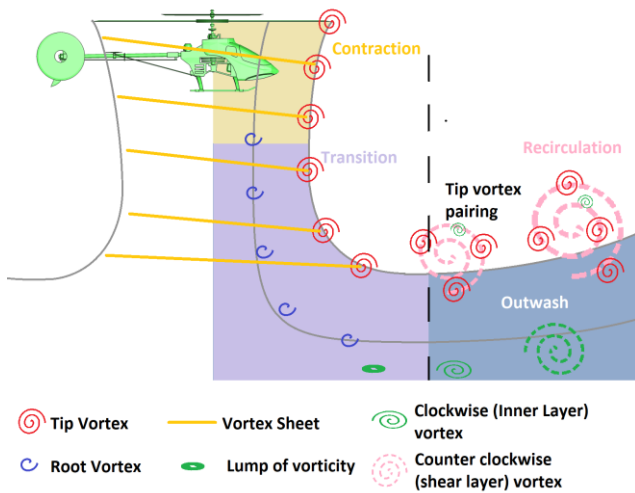


Fig. 2. Scheme of unsteady rotor slipstream (based on Ramasamy et al [8])

However, this picture of the flow is strongly simplified, as its unsteadiness is neglected. In fact, rotor flow is inherently unsteady because of the presence of a finite number of blades. Lifting blades are producing the tip vortices, root vortices, vortex sheets, and oscillations in the inflow (from blade passage). The interaction among these features, as the flow develops, makes the flow field fundamentally unsteady [8]. Moreover, the flow becomes aperiodic because of the self- and mutually induced effects of the strong blade tip vortices [1]. Moreover, the flow becomes aperiodic because of the self- and mutually induced effects of the strong blade tip vortices [1].

The unsteadiness of slipstream itself becomes even more significant in proximity of ground. In this case tip vortices, which flow helically from blade tips, tend

to merge and grow in the outwash area due to friction. It has been sketched in Fig. 2. In the boundary layer of the ground, in the outwash zone, a flow separation bubble may also appear. Separation bubbles are created when the static pressure reaches a minimum directly underneath the vortex flow, and then the developing boundary layer faces a steep adverse pressure gradient downstream of the vortex because of the slower moving fluid. This pressure gradient can become strong enough to produce localized flow separation and the formation of a separation bubble [5]. It has been schematically explained in Fig. 3.

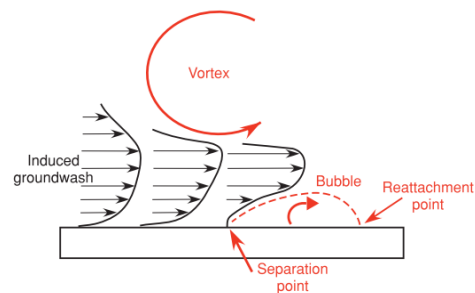


Fig. 3. Creation of vortex-induced separation bubble [5].

As a result, the design of elevated heliports must utilize the unsteadiness of the slipstream in the ground effect, as the oscillating slipstream acts on the heliport plate and causes vibration of building's structure [6]. Some designers claim that the unsteadiness of slipstream should be treated, during design of the heliport, as more important than the steady influence of the helicopter on the building, including its weight and time-averaged slipstream [12]. However, most of the previous studies dealing with pressures in the rotor wake do not consider its unsteadiness. On the other hand, articles focused on unsteady vortical phenomena in the slipstream in the ground effect usually neglect the loads acting on the surface underneath. As a result, to the author's best knowledge, very few publications can be found in the literature that discuss the issue of oscillations of aerodynamic loads acting on the heliport, including its amplitude and frequency. Moreover, the quantitative parameters of the oscillations should be linked with qualitative picture of the flow to indicate main sources of the unsteadiness.

2. EXPERIMENTAL SETUP

The investigation presented in the paper was aimed on estimation of the unsteady loads acting on the heliport. Within the investigation the remotely controlled helicopter T-REX 450 has been utilized. The rotor diameter of this helicopter was 0.71 m

(2.33 ft), and its revolution speed was 2100 RPM. The helicopter rotor was placed above the flat plate, which simulated the heliport's deck (Fig. 4). The plate was equipped in pressure taps, plugged with flexible tubing to the ESP-32HD-DTC multichannel pressure scanner. The rotor thrust and torque was measured by a 6-component strain-gage balance mounted underneath the helicopter's fuselage. Additionally, an optical tachometer has been utilized to measure the rotor revolution speed. The results have been gathered with a PC computer and the in-house software written in LabVIEW environment. The values of pressure measured on the deck surface have been nondimensionalized by referring to the rotor disc loading:

$$(1) \quad C_p = \frac{p - p_{atm}}{\Delta p}$$

where:

p – pressure measured on the deck

p_{atm} – atmospheric (ambient) pressure;

Δp – rotor disc loading

For each measurement a 5-second range of steady conditions have been extracted. The mean value of pressure coefficient $\overline{C_p}$ has been exploited as a metrics of averaged (steady state) impact of the rotor slipstream on the heliport. Respectively, the standard deviation of pressure coefficient, $s(C_p)$, is the metrics of the unsteady impact on the heliport.



Fig. 4. The investigated helicopter T-REX 450 over the simulated heliport

3. RESULTS

Fig. 2 presents exemplary pressure coefficients as a function of azimuth angle, collected during consecutive rotor revolutions roughly in the middle of rotor radius ($r/R=0.56$). Upper chart presents data collected for the hover altitude of $0.5R$ (where R denotes rotor radius) and the lower one – for $1.0R$. In both cases rotor pitch angle was 9° and rotor revolution speed was 2182RPM, which corresponds to thrust coefficient value (out of

ground effect) of $C_{T_{OGE}} = 0.0034$. The unsteadiness of pressure coefficient is clearly visible in both cases, however for the lower flight altitude the C_p is related mostly with rotor azimuth position. Two peaks of C_p for each revolution are caused by the wake of each blade. Meanwhile, increase of the flight altitude makes the time variation of the pressure clearly more significant.

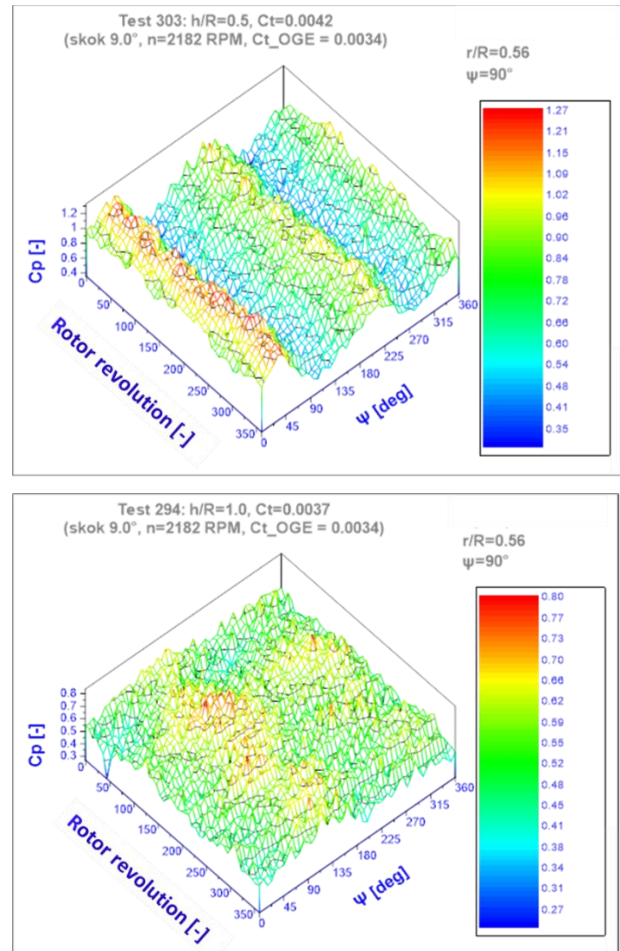


Fig. 5. Pressure coefficient acting on the heliport surface, for the hover altitude of $0.5R$ (above) and $1.0R$ (below).

The impact of rotor height is more evident in results of Fast Fourier Transform, covering respective pressure taps and performed for three different positions of the helicopter above the ground (Fig. 6). Frequencies of the harmonics were referred to the revolution frequency. As it could be expected, the significant peak appeared on the value of $f/f_R = 2$, which means: two times per revolution. Clearly it is the effect of blades' wake passage. The abovementioned peak for the hover height of $0.5R$ is visible in whole investigated spatial area and clearly dominates. However, as the hover

altitude increases, the impact of blades passing frequency decreases. Instead, one may observe that the low-frequency components (roughly, below $f/f_R = 0.25$) become more pronounced in the outer area, for radial location $r/R > 0.5$.

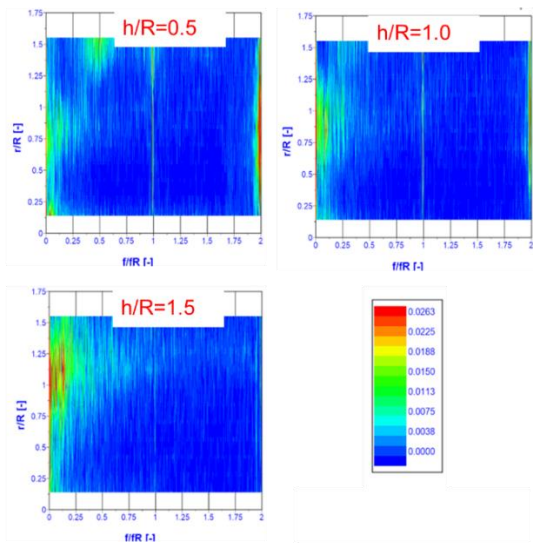


Fig. 6. Results of FFT transformation of pressure coefficient, for hover altitude of 0.5R (upper-left), 1.0R (upper-right) and 1.5R (lower-left)

As it was shown in Fig. 6, the aerodynamic loads acting on the heliport have the dominant frequency equal to the blades passing frequency. However, this statement remains valid only when the hover height is about 1.0R or less. On the other hand, increase of hover altitude increases the impact of low-frequency components. What should be underlined, this change is not reflected in the amplitude of oscillations.

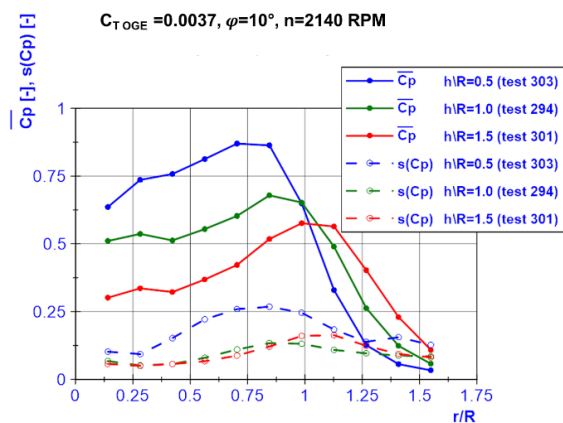


Fig. 7. Radial distribution of mean value of pressure coefficient $\overline{C_p}$ (solid lines) and its standard deviation $s(C_p)$ (dashed lines). Different values of hover altitude, $C_{T OGE} = 0.0037$.

As a metrics of the unsteadiness of pressure, one may utilize the standard deviation of C_p gathered within a 5-second logging. Similarly, the mean value of pressure coefficient $\overline{C_p}$ is a metrics of time-averaged loads. Radial distributions of these parameters, for three values of hover height, have been presented in Fig. 7 (solid lines for $\overline{C_p}$ and dashed lines for $s(C_p)$).

The maximum value of $s(C_p)=0.25$ has been observed, which means that the standard deviation of the pressure may be a quarter of rotor disc load. Such amplitude is significant when compared to the mean value of pressure coefficient, which achieves the maximum of $\overline{C_p}=0.85$.

What must be mentioned, the amplitude of pressure oscillations $s(C_p)$ is the greatest for the lowest value of height, which is intuitive. However, the amplitude not always decreases with the increment of height. Fig. 7 clearly shows that for the height of 1.5R slightly higher values of pressure oscillation amplitude have been registered, than in case of 1.0R. The change is not evident, despite significant change of frequency spectrum: for the higher height, the harmonic component related with blade passing frequency fades out, as it was shown in Fig. 6.

One also should note that the location of the area, where peak values of equivalent amplitude of pressure oscillations changes – however it is strongly related to location of maximum pressure coefficient. As the hover height increases, the point of maximum loads shifts towards the blades tip, which confirms observations by other researchers [4]: [11].

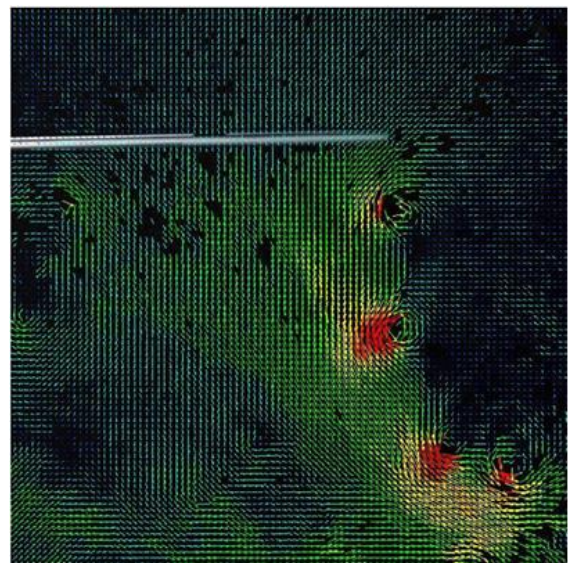


Fig. 8. Velocity field captured with PIV. Tip vortices visible as areas of increased velocity magnitude.

The experiment also included a measurement of the flow field in the proximity of the tip vortices, which can be assumed as a boundary of rotor slipstream. To observe the behavior of tip vortices, the PIV (time-resolved) method has been exploited. A series of frames has been recorded and analyzed to capture location of tip vortex cores, identified as local maxima of the vorticity. Sample results have been presented in Fig. 8 and Fig. 9. The hover altitude was $1.0R$ and thrust coefficient OGE was $C_{T\ OGE} = 0.0037$.

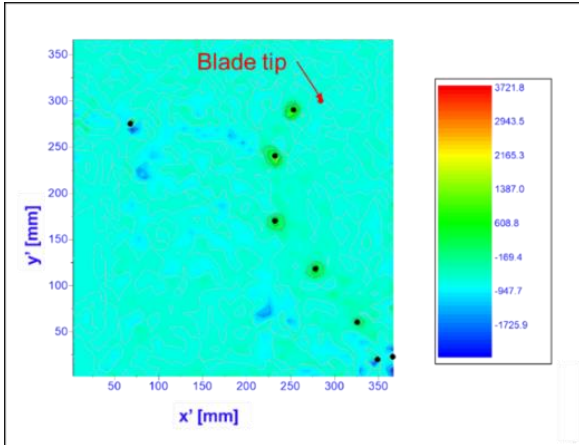


Fig. 9. Location of the tip vortices (black dots) versus blade tip (red dot). Tip vortex from the paddle found in upper-left part of the plot.

The tip vortices captured in different frames (100 frames have been recorded) demarcate an average vortex trajectory, which resembles an Archimedean spiral; this line has been marked in Fig. 10 as a red curve. The coefficients of the spiral were obtained using least square method, when the position of vortices is defined in the polar coordinate system located on the blade tip:

$$(2) \quad \begin{cases} \xi = 736.43 \cdot \frac{a}{R} - 40.74 & \text{for } \frac{a}{R} \leq 0.06 \\ \xi = 38.91 \cdot \ln(15.625 \frac{a}{R}) & \text{for } \frac{a}{R} > 0.06 \end{cases}$$

where $\frac{a}{R}$ is the distance from the blade tip and ξ is the angular position (referred to horizontal direction), calculated using the Cartesian coordinates with the formula:

$$(3) \quad \xi = \arctg\left(\frac{z-z_{tip}}{r-r_{tip}}\right) + 180^\circ \cdot k$$

The factor k takes on the value of 0 or 1 to correctly reflect left and right half-planes.

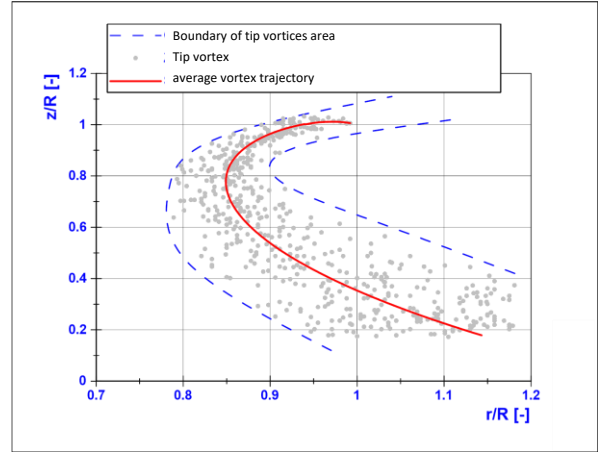


Fig. 10. Average vortex trajectory (red line) and identified tip vortices (grey dots)

Further analysis showed that the vortices found close to the blade tip are located close to their average trajectory. However, as the wake age (and thus the distance between the vortex and blade tip) increases, the position of vortex varies more intensively. The discrepancy of vortices position seems to be periodic, which suggests a logical relation with the low-frequency components presented in Fig. 6. However further studies are required to describe this phenomenon and its sources in more detailed way – likely, it is the flow separation bubble, that appears in the outwash area.

4. SUMMARY

The unsteadiness of the rotor slipstream is an underrated issue, which can play a key role in case of elevated heliports. The slipstream is known as a major source of heliport's vibration, which in line may significantly limit the application of the building underneath the heliport – especially in cases of medical buildings, with the surgeries inside. Despite of this, the amplitude of oscillation of pressure acting on the heliport due to the slipstream seems unknown.

To investigate the topic of unsteady loads acting on the heliport, an experimental investigation focused on a remotely controlled, 450-class helicopter, has been performed. Measurement of pressure acting on the simulated heliport plate showed a level of pressure oscillations for different test cases, as a function of radial position. The maximum value of $s(C_p)=0.25$ has been observed, which means that the standard deviation of the pressure may be a quarter of rotor disc load. Such amplitude is significant when compared to the mean value of pressure coefficient, which achieves the maximum of $\overline{C_p}=0.85$. The point of maximum amplitude is located close to the point of maximum

mean load, regardless the hover height. The dominant frequency of the pressure oscillation depends on the hover height: for the lowest value, the blade passing frequency is crucial, however its impact reduces as the height increases. Instead, the low-frequency components become more significant. It was also observed that the boundary of the slipstream (demarcated by position of tip vortices) varies in time and the discrepancy increases with the wake age. The variation seems periodic rather, than random, however further studies are required to fully explain this observation.

zjawiska konwekcji na pole przepływu.” *Transactions of the Institute of Aviation*, 194–195(3–4), 166–170.

- [11] Tanner, P. E., Overmeyer, A. D., Jenkins, L. N., Yao, C.-S., and Bartram, S. M. (2015). “Experimental investigation of rotorcraft outwash in ground effect.” *71 American Helicopter Society Forum*, Virginia Beach.
- [12] Wąchalski, K. (2016). “Ocena uwarunkowań konstrukcyjnych wyniesionych lądowisk dla helikopterów na budynkach szpitalnych realizowanych obecnie w Polsce.” *Transactions of the Institute of Aviation*, 244(3), 179–191.

5. REFERENCES

- [1] Bhagwat, M. J., and Leishman, J. G. (2000). “Stability analysis of helicopter rotor wakes in axial flight.” *Journal of the American Helicopter Society*, 45(3), 165–178.
- [2] Dziubiński, A. (2016). “CFD analysis of rotor wake influence on rooftop helipad operations safety.” *Transactions of the Institute of Aviation*, 242(1), 7–22.
- [3] Dziubiński, A. (2016). “CFD analysis of wind direction influence on rooftop helipad operations safety.” *Transactions of the Institute of Aviation*, 242(1), 23–35.
- [4] Fradenburgh, E. A. (1972). “Aerodynamic Factors Influencing Overall Hover Performance.” *AGARD Conference on Aerodynamics of Rotary Wings, Proceedings No. AGARD-CP-111*, Marseille, 7-1-7–11.
- [5] Johnson, B., Leishman, J. G., and Sydney, A. (2010). “Investigation of sediment entrainment using dual-phase, high-speed Particle Image Velocimetry.” *Journal of the American Helicopter Society*, 55(4), 42003-1-42003–16.
- [6] Mejsner, M. (2011). “Heliports dangerous for structure of buildings (in Polish: Heliporty groźne dla konstrukcji budynków).” *Administrator24*.
- [7] *PN-B-02171 standard. Estimation of impact of vibration on people in buildings (in Polish: Ocena wpływu drgań na ludzi w budynkach)*. (2017g).
- [8] Ramasamy, M., Potsdam, M., and Yamauchi, G. K. (2015). “Measurements to understand the flow mechanisms contributing to tandem-rotor outwash.” *71 American Helicopter Society Forum, Virginia Beach, VA, USA*, Virginia Beach, VA.
- [9] Smith, A., Bell, A., and Hackett, D. (2017). “Trade-offs in helipad sitting&design.” Rowan Williams Davies & Irwin Inc. (RWDI).
- [10] Świdorski, K. (2008). “Modelowanie numeryczne opływu budynków. Wpływ